

Production of a large diameter electron cyclotron resonance plasma using a multislotted antenna for plasma application

Yoko Ueda, Masayoshi Tanaka,^{a)} Shunjiro Shinohara, and Yoshinobu Kawai
Interdisciplinary Graduate School of Engineering Sciences, Kyushu University, Kasuga, Fukuoka 816, Japan

(Received 5 June 1995; accepted for publication 31 August 1995)

An electron cyclotron resonance plasma with large diameter, uniform, and high electron density is produced using a multislotted antenna. The uniformity of the plasma is within 5% over 20 cm in diameter. The electron density of the helium plasma in front of a substrate is $7 \times 10^{10} \text{ cm}^{-3}$, while the electron density without the substrate is higher than the cutoff density for 2.45 GHz. The effect of the magnetic field configuration on plasma uniformity is investigated. Both of the *R* wave (electron cyclotron wave) and *L* wave are found to be excited in the plasma. © 1995 American Institute of Physics.

I. INTRODUCTION

An electron cyclotron resonance (ECR) plasma¹⁻⁷ has been actively used for plasma processing such as chemical vapor deposition (CVD), etching, and so on. The main reasons are the following: (1) high electron density and adequate high electron temperature, (2) low ion energy, (3) electrodeless plasma production, (4) high speed of deposition of thin films and high speed etching, and (5) possibility to create a compact good-quality film with new properties at such low substrate temperatures as about or below 300 °C. In fact, high deposition rates in the CVD using ECR plasmas were obtained.¹⁻³ However, the recent trend of making larger sized and more precise devices for plasma processing in industry has caused a lot of new problems. Especially important is to generate a uniform and large diameter ECR plasma suitable for a wafer of 20 cm in diameter. An ECR plasma is usually produced with the microwave of the principal mode of wave guides TE₁₀ or TE₁₁, so it is hard to realize a uniform and large diameter ECR plasma. There are few reports⁴ on the production of such a large diameter uniform ECR plasma using magnetic coils, although attempts have been made.

We succeeded in the production of a large diameter ECR plasma using a multislotted antenna (MSA)⁵⁻⁷ which has an advantage that the plasma diameter does not depend on the frequency of the incident microwave. The model of ECR plasma production using MSA⁷ was as follows: MSA with *N* slots can be regarded approximately as an assembly of *N* thin slot antennae.⁸ The electric field radiates from MSA points to all θ directions and accelerates electrons, producing an ECR plasma. MSA is essentially the same antenna as the Lisitano coil⁹ which was developed for the production of a small diameter plasma. We have utilized the Lisitano coil whose diameter is enlarged to produce a large diameter ECR plasma suitable for a wafer of 20 cm in diameter (MSA).

In this paper, we report the experimental results on the production of a large diameter uniform ECR plasma for plasma application with MSA. In Sec. II, the experimental

apparatus is presented, and Sec. III provides the experimental results and discussion. We also investigated in detail the effect of the magnetic field configuration on plasma uniformity. Finally, electromagnetic waves in the plasma were measured with a loop antenna movable along *z* axis and wave patterns were obtained by interferometry in order to examine whether normal modes in the plasma exist or not.

II. EXPERIMENTAL APPARATUS

A schematic of the experimental apparatus is shown in Fig. 1. The vacuum chamber was made of stainless steel having a 29 cm i.d. and 120 cm in length. The magnetic-coil assembly consisted of six coils: four produced a uniform magnetic field, while two others formed the magnetic mirror. The frequency of the microwave was 2.45 GHz and the power varied up to 1000 W. Matching between the microwave circuit and the plasma was adjusted with a stub tuner in such a way that reflected microwave powers as low as possible. An ECR plasma was produced with MSA which was made of stainless steel of 28 cm in diameter. As seen in Fig. 2, the length and width of the slots were 7 and 0.2 cm, respectively.

Helium or Ar was introduced with a typical pressure of 2×10^{-4} Torr. In this experiment, a substrate was placed at 80 cm from MSA (*Z*=100 cm). The diameter of the substrate holder was 27 cm, which enabled a wafer of an 8 in. diam to be held.

In discussing a large diameter plasma, it is important whether or not a substrate is placed in the chamber, because the plasma may be disturbed by the substrate. Here we examined plasma uniformity by measuring the parameters of the ECR plasma in the presence of a substrate having an 8 in. diam. Plasma parameters were measured with a cylindrical Langmuir probe made of a 0.1 cm diam tungsten wire extending 0.3 cm from a ceramic insulator. The probe was inserted radially into the chamber to minimize the disturbance to the probe characteristics.¹⁰ It was also reported¹⁰ that the plasma density in magnetized plasmas inferred from the probe measurements is likely to be a factor of 2-4 lower due to the combination of the magnetic fields and Debye length effects. We also observed⁵ that the plasma density is a little

^{a)}Also at National Institute for Fusion Science, Chikusa-ku, Nagoya 464-01, Japan.

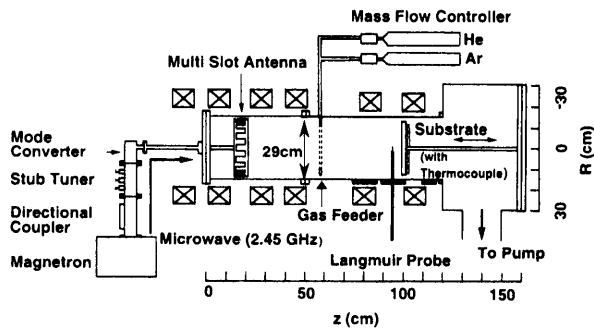


FIG. 1. Schematic diagram of the experimental apparatus.

low compared to that measured with a microwave interferometer. This may be due to the fact that the effective area of the probe inserted perpendicularly to magnetic fields becomes about half, when plasmas flow along the magnetic field lines.

The determination of the electron temperature (T_e) is difficult. For this reason, we focused our attention on characterizing the ion saturation current density (I_{is}) as a function of operating conditions. Nevertheless, T_e was derived from the best fit curve for the Langmuir probe characteristics which was the semilog plot of the electron current versus the probe potential (V_p).¹¹ The ion density (=electron density N_e) was determined¹¹ from the ion saturation current density using the standard thin probe theory since the probe radius (r_p) is much larger than the Debye length (λ_D); that is, the ion sheath is thin. In this case, nearly all particles reaching the sheath boundary are absorbed by the probe. According to the theory,¹² a cylindrical probe current consists of both the sheath limited current and the orbit limited current. In this case where sheath limitation of particle motion prevails, the probe current is reduced to the corresponding expression for a plane probe.¹² Hence I_{is} is independent of V_p and is saturated. Thus, for $r_p \gg \lambda_D$, assuming electrons with Maxwellian energy distribution, the ion density is given by

$$N_i = 1.6 I_{is} e^{-1} (m_i / k T_e)^{1/2}, \quad (1)$$

where e is the electron charge. In addition, when the ion Larmor radius (about 0.6 cm for $T_i = 1$ eV and $B = 500$ G) is larger than r_p and λ_D , magnetic fields will not affect the ion saturation current so much. Thus we used Eq. (1) to determine the electron density ($N_e = N_i$).

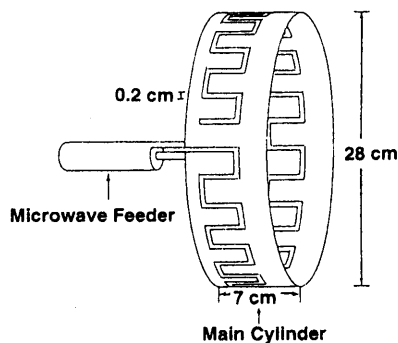


FIG. 2. Schematic view of the multislot antenna.

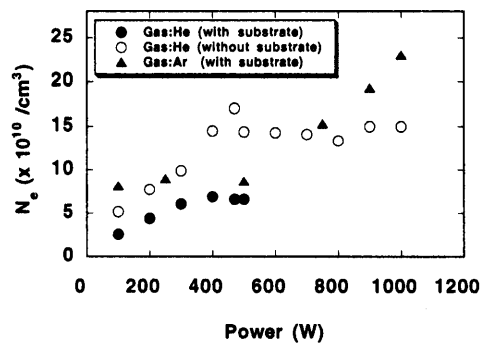


FIG. 3. Dependence of the electron density on the incident microwave power. The used gas is He or Ar with a pressure of 2×10^{-4} Torr.

Electromagnetic waves in the plasma were measured with a loop antenna movable along the z axis and the wave patterns were obtained by interferometry as usual.¹³ The amplitude of wave patterns were given with arbitrary units because of using a loop antenna which was not calibrated. The power meter which is a thermometric type was used to measure the spatial profile of the power of microwaves.

III. RESULTS AND DISCUSSION

The value N_e was measured to investigate what high electron densities could be obtained with MSA. Figure 3 shows a dependence of N_e on the incident microwave power for different gases, Ar and He. This figure shows that N_e becomes higher than the cutoff density ($7 \times 10^{10} \text{ cm}^{-3}$) for 2.45 GHz, and N_e in the absence of the substrate is approximately two times larger than that in the presence of it.

In order to search an optimum condition for a uniform plasma, the radial profile of I_{is} was measured as a function of input microwave power, gas pressure, and magnetic field configuration. It was found that a uniform plasma is obtained using MSA under the limited experimental conditions. Figure 4(a) shows the radial profile of I_{is} when the incident microwave power and the gas pressure were 470 W and 2×10^{-4} Torr (He gas), respectively. Figure 4(a) shows that the uniformity of the radial profile of I_{is} is within 5% over 20 cm in diameter. The electron density and electron temperature, which were measured at 5 cm from the substrate, were $7 \times 10^{10} \text{ cm}^{-3}$ and 6 eV, respectively. In this experiment, the ionization degree is estimated to be $\sim 1\%$, which means that MSA is an efficient antenna for ECR plasma production.

Figure 4(b) shows the radial profile of the floating potential (V_f) in the case of the uniform plasma. The uniformity of V_f is ± 0.75 V over 20 cm in diameter. The value V_f is slightly positive although V_f , in the case where the radial profiles of I_{is} were not uniform, was in the range from -5 to -20 V, which means that there were few high energy electrons for the uniform plasma.⁵ The uniformity of the radial profile of V_f is very important for plasma processing. It is well known that some problems for plasma processing are caused by the condition that V_f is not uniform. For etching, one of the problems is so-called "charge up"—an electric field is generated on the surface of insulating films and

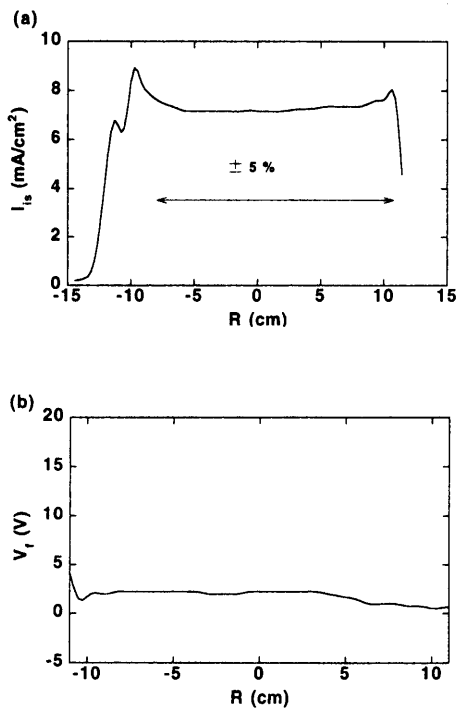


FIG. 4. Radial profiles of (a) the ion saturation current density and (b) the floating potential for the case of the uniform plasma. The incident microwave power and gas pressure were 470 W and 2×10^{-4} Torr, respectively.

causes destruction of the films. Therefore, the result of Fig. 4(b) suggests that a large diameter uniform plasma suitable for plasma processing was generated.

Since magnetic fields generally play an important role in the behavior of plasmas, two-dimensional axial magnetic field lines are calculated. As seen in Fig. 4(a), the ECR plasma decays at positions $R = \pm 12$ cm, which is understood by the fact that the plasma flows along the magnetic field lines in Fig. 5. The magnetic field is stronger near the chamber wall, and the plasma outside the peaks dies out because recombination occurs at the point where the magnetic field lines cross the wall of the chamber. Thus, it is expected that larger diameter uniform ECR plasmas having more than an 8 in. diam will be obtained by MSA if the chamber is enlarged.

The radial profiles of the ion saturation current changed remarkably depending on incident microwave powers, gas pressures, and magnetic field configurations.¹⁴ In order to investigate the effect of magnetic fields on plasma uniformity in detail, the radial profiles of I_{is} were measured changing the gradients of magnetic field intensity (∇B) at the ECR point as well as the ECR points. Axial magnetic field configurations when ∇B was changed are illustrated in Fig. 6(a), where ∇B was -4 , -27 , and -55 G/cm. In this case, the ECR point was kept at the same position $Z = 33$ cm. Figure 6(b) shows the radial profiles of I_{is} corresponding to the cases of Fig. 6(a), where the incident microwave power was kept at 470 W. The uniform plasma was obtained when ∇B was -27 G/cm. As shown in Fig. 6(b), the ion saturation current density in the case of $\nabla B = -55$ G/cm is low at the center and high at the side; that is, the radial profile of I_{is} shapes concave. On the other hand, the radial profile of I_{is} in the case where ∇B is -4 G/cm shapes convex. Figure 7

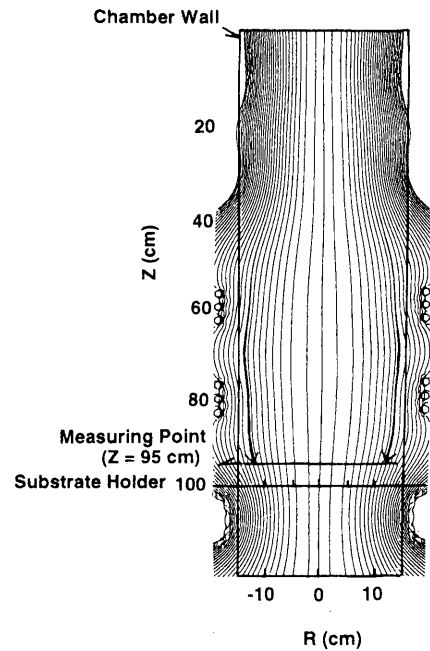


FIG. 5. Two-dimensional magnetic field lines corresponding to the magnetic field configuration in Fig. 4.

shows the dependence of N_e on ∇B . This figure indicates that N_e increases as ∇B is increased, which is similar to the case of ECR plasma production with the microwave of the principal mode of waveguides.⁴

Figure 8(a) illustrates axial magnetic field configurations for different ECR positions. The ECR points were set inside MSA ($Z = 14$ cm) and at the positions of 4, 13, and 23 cm

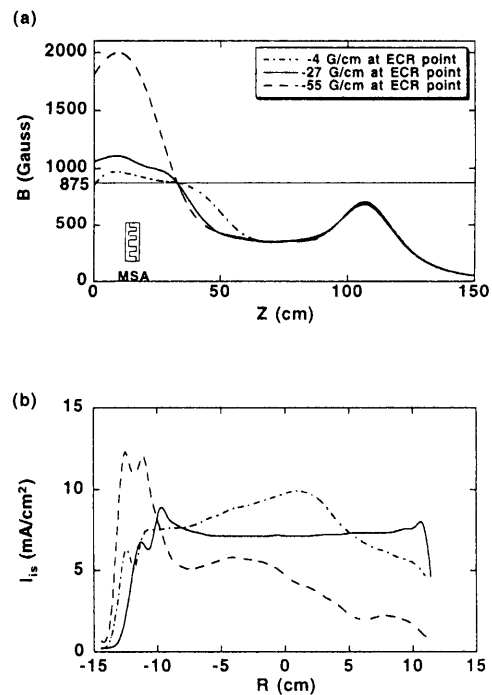


FIG. 6. (a) Axial profiles of magnetic fields at the center when ∇B at the ECR point is changed. (b) Radial profiles of the ion saturation current density for different ∇B values.

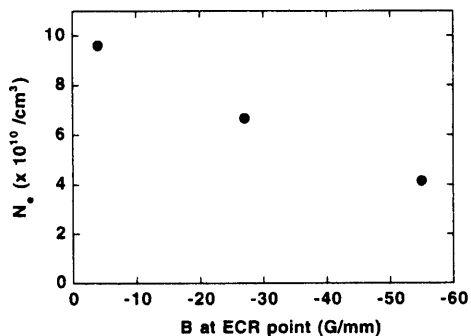


FIG. 7. Dependence of the electron density on ∇B at the ECR point.

from MSA ($Z=24, 33,$ and 43 cm), where ∇B was kept at -27 G/cm. Figure 8(b) shows the radial profiles of I_{is} in the magnetic field configurations corresponding to Fig. 8(a). Although I_{is} in the case where the ECR point was set outside MSA was two times larger than that inside MSA, I_{is} did not depend on the ECR position as long as it was set outside MSA.

Usually, an ECR plasma has been produced by two methods: resonant acceleration of electrons by electric fields, and interaction between plasma waves and electrons. The mechanism of the production of an ECR plasma using MSA was already described in Sec. I. However, N_e was higher than the cutoff density as seen in Fig. 3. It was also found that the uniformity of the radial profile of I_{is} depends greatly on magnetic field configurations, and I_{is} axially increases after the resonance point under the certain magnetic field profiles.¹⁴ These results suggest that there may exist normal

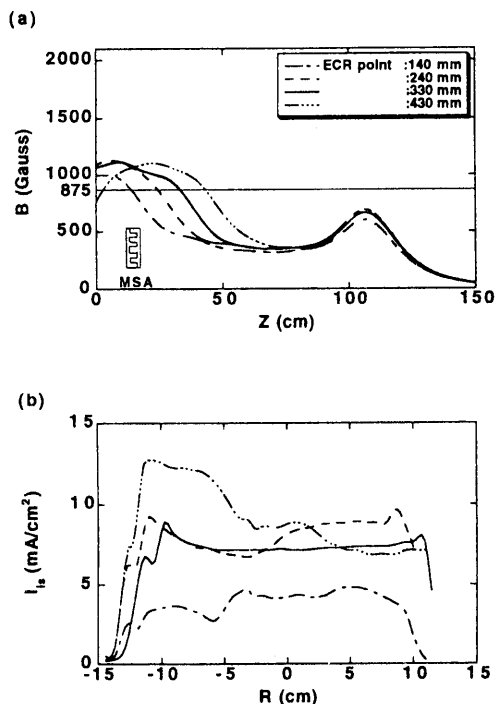


FIG. 8. (a) Axial profiles of magnetic fields at the center when the ECR points are changed. (b) Radial profiles of I_{is} for different magnetic field configurations.

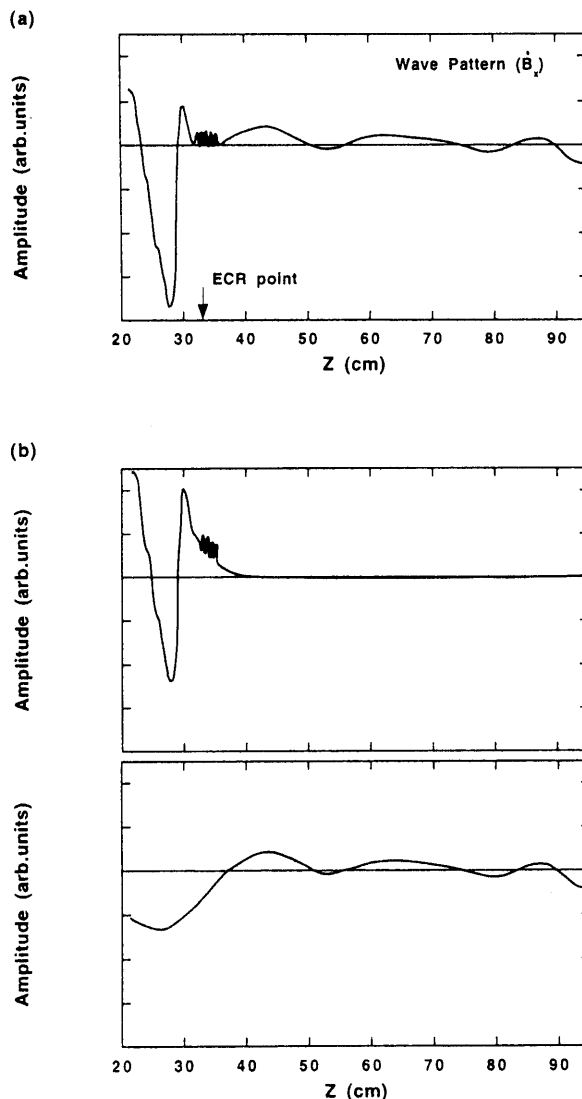


FIG. 9. (a) Wave pattern of B_x in the case of the uniform ECR plasma. (b) Wave patterns decomposed graphically from B_x .

modes relating to the plasma production such as electron cyclotron waves.

Electromagnetic waves in the plasma were measured with a loop antenna in order to clarify the dependence of the radial profiles of I_{is} on the magnetic field configurations from the point of view of plasma production. Furthermore, it was examined by measuring the dispersion relation of electromagnetic waves whether normal modes in the plasma exist or not. Figure 9(a) shows a typical interferometric wave pattern of B_x in the uniform plasma. As seen in Fig. 9(b), the wave pattern was decomposed graphically into two traces assuming that it consisted of two waves with different wave numbers. In addition, we confirmed that the sum of the two traces was nearly equal to the original interferometric wave pattern. Figures 10(a) and 10(b) show the dispersion relations before the ECR point and after the ECR point, respectively. The solid lines in Fig. 10 are the theoretical dispersion curve.¹⁵ Here, the local wave numbers were estimated¹³ from the wave patterns in the regions between the MSA and the ECR point and after the ECR point in Fig. 9(b). They were

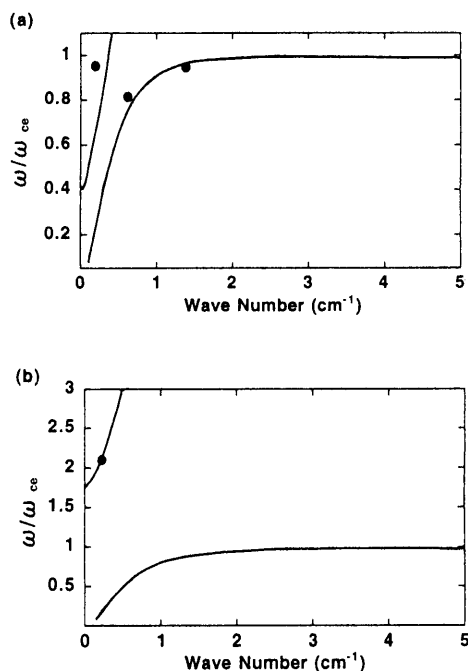


FIG. 10. Dispersion relations (a) before the ECR point and (b) after the ECR point.

plotted in Fig. 10 using the local field intensity. Figure 10 indicates that the R wave (electron cyclotron wave) and the L wave¹⁵ propagate in the region between the MSA and the ECR point, and the only L wave propagates after the ECR point. According to the theoretical dispersion curve, the L wave does not propagate if N_e is higher than about $2 \times 10^{11} \text{ cm}^{-3}$ in this experiment. The L wave damped as the gas pressure was increased, and the damping rate of the L wave

was comparable to the inverse of the mean free path of electron collisions. There may be a possibility that the L wave suffered from collisional damping. The output of the power meter had different axial profiles depending on the experimental conditions. Although the model of the production of an ECR plasma using MSA was as described in Sec. I, it seems that absorption of electromagnetic waves was connected to the uniformity of the ECR plasma as well as the plasma production. More detailed experiments such as measurements of spatial wave patterns will be necessary for clarifying whether R and L waves contribute to the production and uniformity of the plasma or not.

- ¹ S. Mastuo and M. Kiuchi, *Jpn. J. Appl. Phys.* **22**, L210 (1983).
- ² M. Kitagawa, K. Setsune, Y. Manabe, and T. Hirao, *Jpn. J. Appl. Phys.* **27**, 2026 (1988).
- ³ Y. Nakayama, M. Kondoh, K. Hitsuishi, and T. Kawamura, *Jpn. J. Appl. Phys.* **29**, 1801 (1990).
- ⁴ S. Samukawa and T. Nakamura, *Jpn. J. Appl. Phys.* **30**, 3147 (1991).
- ⁵ Y. Kawai and K. Sakamoto, *Rev. Sci. Instrum.* **53**, 606 (1982).
- ⁶ A. Yonesu, Y. Takeuchi, A. Komori, and Y. Kawai, *Jpn. J. Appl. Phys.* **27**, 1482 (1988).
- ⁷ Y. Suetsugu and Y. Kawai, *Jpn. J. Appl. Phys.* **23**, 1101 (1984).
- ⁸ E. A. Wolff, *Antenna Theory and Design*, 2nd ed. (Sir Isaac Pitman, London, 1966), Vol. 2, Chap. 7, p. 497.
- ⁹ G. Lisitano, R. A. Ellis, Jr., W. M. Hooke, and T. H. Stix, *Rev. Sci. Instrum.* **39**, 295 (1968).
- ¹⁰ S. M. Gorbalkin, L. A. Berry, and J. B. Roberto, *J. Vac. Sci. Technol. A* **8**, 2893 (1990).
- ¹¹ E. S. Aydil, J. A. Gregus, and R. A. Gottscho, *Rev. Sci. Instrum.* **64**, 3572 (1993).
- ¹² W. Lochte, *Plasma Diagnostics* (North-Holland, Amsterdam, 1968), Chap. 11, p. 679.
- ¹³ M. Tanaka, R. Nishimoto, S. Higashi, N. Harada, T. Ohi, A. Komori, and Y. Kawai, *J. Phys. Soc. Jpn.* **60**, 1600 (1991).
- ¹⁴ Y. Ueda, M. Tanaka, S. Shinohara, and Y. Kawai, *Proceedings of the 7th Symposium Plasma Science for Materials*, Tokyo, 1994 (unpublished), p. 23.
- ¹⁵ F. F. Chen, *Introduction to Plasma Physics and Controlled Fusion* (Plenum, New York, 1977), Chap. 4.